Scanning Microscopy

Volume 4 | Number 4 Article 6

8-29-1990

Cryo-Preparation and Planar Magnetron Sputtering for Low Temperature Scanning Electron Microscopy

T. Müller
Balzers Union AG

P. Walther
University of Wisconsin, Madison

C. Scheidegger
Fed. Inst. for Forest, Snow, and Landscape (WSL)

R. Reichelt
University of Münster

S. Müller
University of Basel

See next page for additional authors

Cryo-Preparation and Planar Magnetron Sputtering for Low Temperature Scanning Electron Microscopy

Authors

T. Müller, P. Walther, C. Scheidegger, R. Reichelt, S. Müller, and R. Guggenheim

Scanning Microscopy, Vol. 4, No. 4, 1990 (Pages 863-876) 0891-7035/90$3.00+.00
Scanning Microscopy International, Chicago (AMF O'Hare), IL 60666 USA

CRYO-PREPARATION AND PLANAR MAGNETRON SPUTTERING FOR LOW TEMPERATURE SCANNING ELECTRON MICROSCOPY

T. Müller*, P. Walther[1], C. Scheidegger[2], R. Reichelt[3], S. Müller[4], and R. Guggenheim[5]

Balzers Union AG, Principality of Liechtenstein
[1]University of Wisconsin, Madison, Wisconsin
[2]Fed. Inst. for Forest, Snow, and Landscape (WSL), Birmensdorf, Switzerland
[3]Inst. Med. Physik, University of Münster, West Germany
[4]MIH at Biocenter, and [5]SEM Laboratory, University of Basel, Switzerland

(Received for publication March 14, 1990, and in revised form August 29, 1990)

Abstract

Cryo-preparation is a reliable technique for the structural investigation of food products in low temperature scanning electron microscopy (SEM). Artifacts, such as, the segregation of water/non-water ingredients, occur during the freezing process by the crystallization of ice; they can be helpful for correct interpretation of visualized details, e.g., the detection of water containing compartments. The size of the segregation structures depends on water concentration and specimen thickness. The condensation of water vapor (ice contamination) is influenced by the specimen temperature and the partial pressure of the water inside the vacuum system. Furthermore, the evaporation (sublimation, etching) of specimen water can be regulated by monitoring the specimen temperature. Sublimation under SEM observation, i.e., "in situ etching" at low acceleration voltage, allows the progress of etching to be observed continuously, prior to the coating of the specimen inside a dedicated cryo-preparation system attached to the SEM. Coating of specimens provides superior structural resolution compared with the observation of uncoated samples. A coating layer of platinum (~ 1-2 nm thick), deposited on a cold substrate by planar magnetron sputtering, is almost homogenous and has a density close to that of the solid metal. Its use allows bulk biological specimens to be observed in low temperature SEM with a structural resolution up to the visualization of transmembrane proteins.

KEY Words: Cryo-preparation, cryo-fixation, freeze-fracture, partial freeze-drying, planar magnetron sputtering, platinum, low temperature scanning electron microscopy, yeast, whipped cream, low-fat dairy spread.

*Address for Correspondence:
T. Müller,
Balzers Union AG,
P.O. Box 75,
FL-9496 Balzers,
Principality of Liechtenstein

Telephone: 41-75-45611
FAX: 41-75-42332

Introduction

Freeze fixation is a technique to rapidly immobilize biological specimens [Plattner and Zingsheim, 1983]. If carried out sufficiently fast, no changes occur in their structural and physiological constitution [Plattner and Bachmann, 1982]. Fast freezing was established as a preparation step, prior to fracturing and replication, in the freeze-etch technique of transmission electron microscopy (TEM) [Moor, 1959, 1971; Steere, 1971]. Many different methods using plunge- [Dubochet et al., 1982], spray- [Bachmann and Schmitt-Fumian, 1971], propane jet- [Müller et al., 1980], copper mirror- or slam- [van Harreveld and Crowell, 1964; Heuser, 1977], and high pressure freezing [Moor and Riehle, 1968; Moor, 1986] are nowadays widely applied [for reviews see: Robards and Sleytr. 1985; Steinbrecht and Zierold, 1987]. Cryo-techniques have also been used in low temperature scanning electron microscopy (LTSEM) for some years, taking advantage of the fact that with these methods, soft and mechanically unstable samples (containing water and other volatile components) can be observed in the LTSEM as frozen bulk specimens [for a bibliography see: Bastacky et al., 1987].

In addition to development and presentation of commercial equipment for cryo-preparation [Robards and Crosby, 1978; Sargent, 1988a; Beckett et al., 1982; Müller et al., 1986, 1988, 1991] various coating techniques have been investigated and different procedures established:

The technique of **planar magnetron sputtering** with different target materials, such as gold, gold-palladium, platinum and several others has been improved [Echlin, 1985]. A finer granularity is reported to occur at a lower specimen temperature [Echlin, 1981] which supports the proposal of earlier authors [Zinsmeister, 1965].

Atom or ion beam sputtering under high vacuum conditions were introduced as alternatives to low vacuum magnetron sputtering or high vacuum evaporation [Jakopic et al., 1978, Peters, 1980]. A reliable signal to noise ratio was obtained with this techniques, giving high resolution micrographs in a field emission SEM [Peters, 1985].

Electron beam evaporation of chromium, using double axis rotary shadowing technique [Hermann et al., 1988],

or platinum-iridium-carbon in high vacuum at -80°C and ultrahigh vacuum at -250°C on freeze-dried test specimens have been analyzed in TEM, SEM and in a scanning tunneling microscope [Amrein et al., 1990]. Another method consists of electron beam evaporation of 2 nm of platinum-carbon at an elevation angle of 45° followed by 10 nm of carbon at 90° (to enhance the electrical conductivity) and using the backscattered signal (which originates mainly at the Pt-C layer which is in close contact with the biological structures of interest) for imaging. Under these conditions masking of specimen fine structure is minimized and membrane particles have been detected on large critical-point dried bulk specimens [Walther and Hentschel, 1989].

In spite of these advanced and some times complex coating techniques we have applied planar magnetron sputtering in a high vacuum chamber, under well defined conditions, to high resolution LTSEM [Müller and Walther, 1989]. It is the aim of this review paper to relate the experience gained from freeze-etching for TEM to the application of a scanning cryo unit attached to a conventional or field emission SEM. Artifacts produced when freezing, freeze-fracturing, etching (partial freeze drying), and sputter-coating biological specimens, e.g., food products in preparation for LTSEM are considered. An extended section deals with the resolution obtainable by planar magnetron sputter coating. Applications for food investigations in moderate and high resolution LTSEM demonstrate the versatility of approach.

Materials and Methods

Scanning Cryo Unit

The scanning cryo unit, Balzers SCU 020, is a dedicated system containing two cold stages aligned for on-line transfer of specimens under high vacuum conditions. The temperature of both stages (preparation chamber and SEM goniometer) can be monitored independently in the range between +50°C and -150°C. The automatic cooling system as well as the turbo molecular pump in the preparation chamber allow this system to be attached to any SEM without microscope modification [for a technical description see: Müller et al., 1991].

Freeze Fixation

Samples ($\sim$ 1 mm^3) for freeze-etching were mounted on gold carrier plates (Balzers) and frozen by plunging into liquid propane (cooled by liquid nitrogen). Under liquid nitrogen, the carriers were then clamped to a specimen table, which was inserted into the SCU 020 against a flow of dry nitrogen gas and mounted on the cryo stage of the preparation chamber cooled to -130°C.

Preparation

Once the preparation chamber was at high vacuum (pressure $<= 2 \times 10^{-6}$ mbar) the cryo stage temperature was raised to -110°C, -105°C, or -100°C for slow etching or to -90°C for deep etching. To retain the samples in the fully frozen hydrated state specimens were kept at -120°C and the sputtering process was started before fracturing. Thus, immediately after creation of the fracture faces, coating was performed and the condensation of water on the sites of interest was correspondingly reduced. Au or Pt sputter coating was carried out at a total pressure of 2.2×10^{-2} mbar obtained by the inlet of pure argon gas. The nominal coating thickness was measured by a quartz crystal thin film monitor (QSG 301, Balzers).

Transfer

After completion of coating, high vacuum was reestablished and the specimens were transferred on-line to the SEM cryo stage. All transfer movements were guided by tracks on the manipulator so, the transfer can be repeated as often as required without necessity of any visual control [Müller et al., 1991]. The goniometer cryo stage was always kept at a temperature below -120°C for reduction of beam damage.

SEM

The scanning electron microscopes used were: Cambridge MK IIa: Fig. 1; Philips SEM 515: Figs. 2 and 5-10, and Hitachi S800: Figs. 3, 4, 11, 16 and 17.

TEM and STEM

For structural characterization by TEM and determination of their thickness by scanning transmission electron microscopy (STEM), test sputter coatings were produced on carbon coated 400 mesh copper grids [Gross et al., 1985]. TEM micrographs were taken in a Siemens CT 150 (at 120 kV) or a Zeiss EM 109 (at 80 kV). Digital dark field micrographs were recorded by the Vacuum Generators HB-5 STEM at 80 kV. The intensity of those STEM micrographs is proportional to the fraction of electrons scattered elastically by the coatings and so provides a direct and precise measure of the mass thickness of the sample [Reichelt and Engel, 1984].

Thickness variations in the horizontal plane of sputter coatings (deposited on glass cover slips) were measured mechanically in a Dektak 3030 scanning instrument (Sloan Techn., Inc., Santa Barbara, CA).

Results and Discussion

Freezing

Unless super-cooled, water crystallizes when cooled below its freezing point. Small molecules and ions lower the freezing point considerably. Therefore, glycerol or sucrose are often used as cryo-protectants. Freezing artifacts, e.g., the segregation of crystallizing water and non-water molecules (previously described as "eutectic material") are dependent on the speed of freezing and on the concentration of the cryo-protectant. There are two approaches to freeze fixation. One is to fix the specimen without any freeze damage, thus having the maximum structural protection. This approach is only applicable to very thin samples [Dubochet et al., 1988]. The other is to accept a certain amount of segregation so that compartments with a high water content may be recognized by the segregation pattern [Brooker, 1988]. Most of the cryo-protectants introduce artifacts, so in general, one should try to immobilize biological specimens in their untreated natural state. Specimen thickness also limits the quality of freezing. For thin specimens (thickness $<= 20$ μm) ultra-rapid freezing by slamming samples onto a polished, cold copper block, or jetting liquid propane onto the surfaces of a specimen sandwiched between two copper plates should be applied. For thick specimens (thickness up to 600 μm) high pressure

freezing is recommended.

Differences in the appearances of segregation, observed in the same specimen after the freezing process, result from different water concentrations in the various cell compartments [see also: Read, 1990]. Fig. 1 shows a wheat leaf infected by the rust fungus Puccinia triticina. The specimen was frozen by plunging into liquid propane, then fractured, etched, coated with 10 nm gold at -90°C, and observed in a SEM at -120°C with 20 kV electrons. Partial sublimation of the crystalline ice may be seen. In the vacuole (V, high water concentration) the ice crystals are larger than in the cytoplasm of the host (EHM) or the parasite (H) [Grabski et al., 1987; Guggenheim et al., 1991]. In addition, in the vacuole clearly a gradient in the size of segregation structures is visible. This indicates that with increasing distance to the surface slower freezing creates larger artifacts. Particle-like structures have been observed in the extracellular space of frozen fixed plant leaves [Jeffree et al., 1987]. From the explanations given, condensation of water vapor during freezing and transfer of the specimen to the vacuum chamber would seem to be the most reasonable. This is supported by the fact that these ice crystals are "cleaned away" by partial freeze-drying (etching).

Low-fat dairy spread (e.g. "Butterfly", Meggle) has a high water content (53% H_2O, 40% fat). In that type of products water (present as droplets) is in the dispersed and fat in the continuous phase [Buchheim, 1982; Buchheim and Dejmek, 1990]. In our hands very often the water compartments revealed by freeze-fracturing have a tube-like appearance (Fig. 2). By partial freeze-drying of the specimen these "water tubes" (WT, Fig. 2) are easy to identify by the segregation pattern.

Freeze-etching

Even in a high vacuum chamber, ice crystals grow on freshly freeze-fractured specimens as a result of water vapor condensation [Gross et al., 1978b]. If a liquid nitrogen cooled Meissner trap (i.e. a cold surface somewhere in the recipient which acts as a cryo pump to H_2O molecules) is present, the partial pressure of water (pH_2O) in the vacuum chamber is approximately 0.5 times the total pressure. The saturation vapor pressure of water ($svpH_2O$) at the surface of a frozen specimen [Honig and Hook, 1960] depends only on the specimen temperature. The ratio condensation / sublimation of water molecules on the specimen surface is determined by the ratio $pH_2O/svpH_2O$. In a high vacuum chamber with a total pressure of 2×10^{-6} mbar the critical condensation temperature is -110°C.

Under these conditions pH_2O and $svpH_2O$ are equal, so at any one time the amount of water, condensing on the specimen surface or subliming from it, is the same. As a consequence, at specimen temperatures below -110°C the rate of condensation is higher than that of sublimation; the result is increased contamination on the specimen surface by water. Quantitative etching can therefore only occur at temperatures above the critical condensation temperature. Provided the vacuum is better than 1×10^{-6} mbar, the speed of etching (lowering the ice level) only depends on the specimen temperature. It is estimated to be about 0.2 nm/s, 2 nm/s, and 20 nm/s at specimen temperatures of -110°C, -100°C, and -90°C respectively [Böhler, 1975].

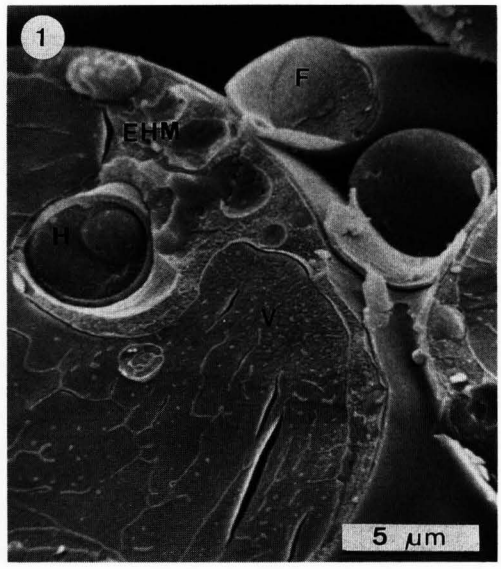

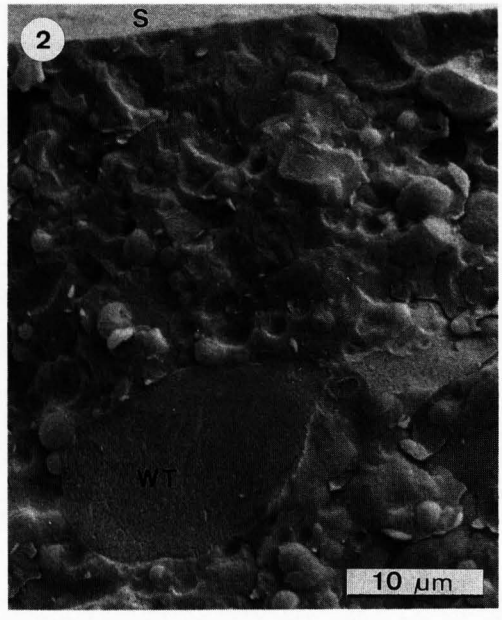

Figure 1. Cross fracture through cells of a wheat leaf infected by the rust fungus Puccinia triticina (F). The fungal haustorium (H), the encasement of the haustorium (EHM) and the vacuole (V) of the host cell exhibit a different size of segregation structures dependent on (i) the H_2O concentration and (ii) on the distance to the cell surface.

Figure 2. Cross fracture through a piece of low fat dairy spread. The recorded area is adjacent to the surface (S) of the specimen. Note the tube-like appearance of the water containing compartment (WT).

A yeast cell suspension, frozen in liquid propane, was fractured and coated at -130°C. The irregular distribution of particles on the plasmatic fracture face (PF) of the plasmalemma (Fig. 3) indicates that the particles are ice crystals.

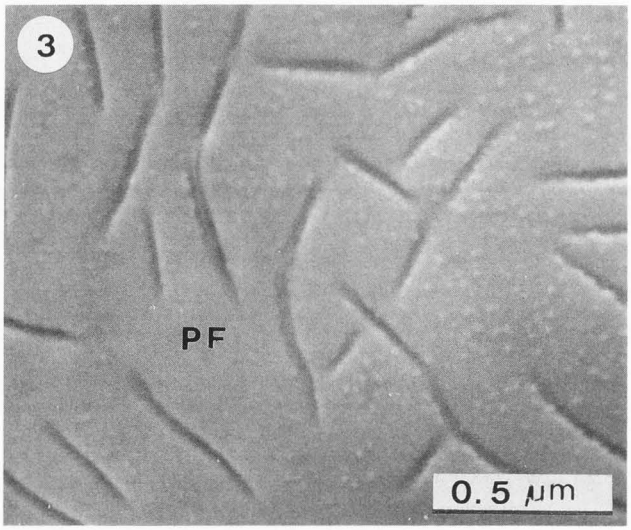

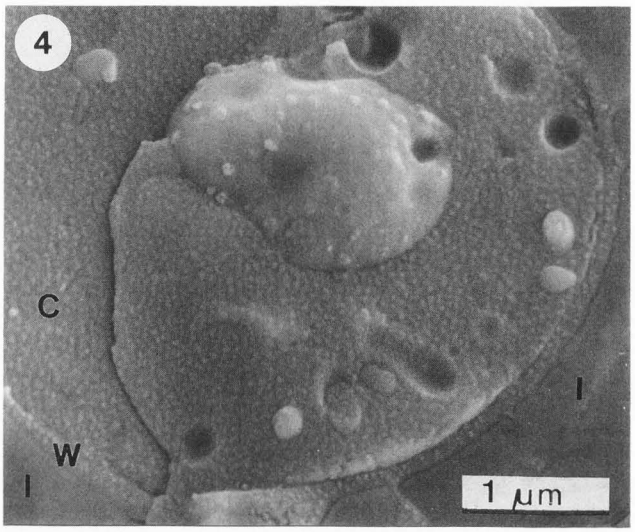

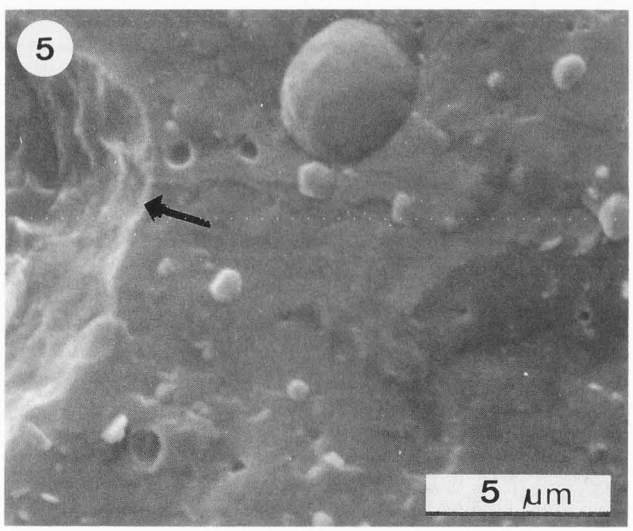

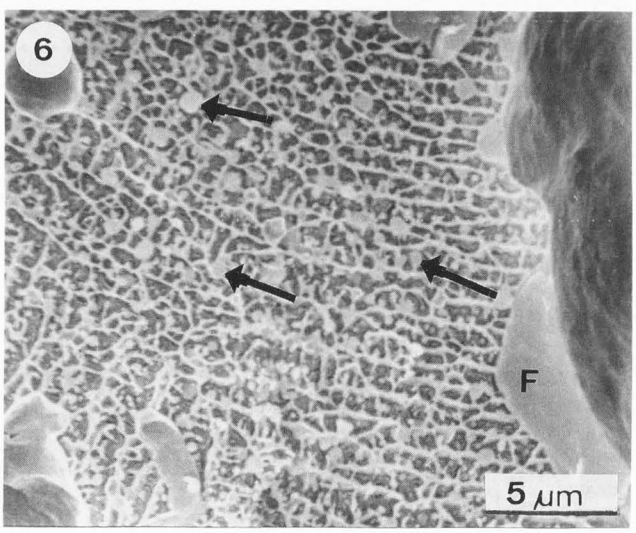

Figure 3. Plasmatic fracture face (PF) of yeast (Saccharomyces cerevisiae) plasmalemma, planar magnetron sputter-coated with 3-4 nm gold. The different size and distribution of particles is due to water condensation between fracturing at -120°C and coating.

Figure 4. Cross fracture through a yeast cell. Water condensation causes a granular appearance of the cytoplasm (C) and the cell wall (W), but the surrounding ice (I) fracture plane is smooth. Fracturing and coating as for Fig. 3.

Figure 5. Cross fracture through whipped cream, fully frozen-hydrated. At the border of the big air cell (arrow) there is no information about the distribution of fat and water.

Figure 6. Cross fracture through whipped cream, partially freeze-dried. Distinct portions of fat (F) can easily be recognized at the border of a big air cell. Many fat droplets (arrows) can be seen in the eutectic between the ice crystals.

In the cross fracture of a yeast cell (Fig. 4), the rough appearance of the fracture plane of the cytoplasm and the cell wall is also due to water contamination. In both cases, the specimen temperature was too low, so heavy contamination occurred during the time span between fracturing and coating. The water layer and the ice crystals are stabilized by the coating and cannot be removed by raising the specimen temperature after the coating process. Contamination is much reduced for specimens fractured at a temperature close to the critical condensation temperature of water. Coating and fracturing have to occur simultaneously. It is thus possible to achieve fractures of fully frozen hydrated specimens

with only little or virtually no contamination. A portion of whipped cream plunge frozen in liquid propane, was fractured at -120°C (Fig. 5). Apart from one big air cell (arrow), concave and convex structures (small air cells or fat droplets) are embedded in a more or less smooth matrix. No contamination products are visible in the air cells, no particles can be recognized on their walls. In an earlier experiment, the same sample had been fractured at -100°C and etched for 5 minutes (Fig. 6). Again, no particles are visible on the walls of the air cells. This indicates the absence of small fat droplets at the air-water interface. The matrix is not uniform. Since only pure water sublimes from the cross fracture of the matrix, the segregation pattern observed in this region is that of ice and cream; several fat droplets of a similar size can be identified (arrows). In addition, large fat portions (F) which seem to stabilize the air cells are clearly identified. The specimen was not removed from the vacuum system between these two fracturing experiments. In view of such different results, achieved with the same specimen, it should be noted that:

a) Sublimation only takes place at the surface or fracture face of a specimen. The material below remains fully frozen hydrated. This indicates excellent thermal contact. Otherwise, it would not have been possible to further cool the specimen for the second frozen hydrated experiment.

b) Segregation pattern can only be visualized by etching (the history for Figs. 5 and 6 was the same); frozen hydrated specimens may contain segregation patterns even if these are not visible. So etching is a useful tool for the detection of segregation artifacts and important for correct interpretations (e.g., identification of small fat droplets in Fig. 6).

In Situ Etching

When freeze-etching for TEM, it is essential to monitor the etching depth (see freeze-etching). In the SCU 020, freeze-fracturing is carried out in a preparation chamber which is attached to a SEM. As the system provides the SEM with a cryo-stage, it can be used for high vacuum cryo-transfer; spruce needles of Picea abies (Fig. 7, also compare to Fig. 8) and portions of low-fat dairy spread (Fig. 9, also compare to Fig. 10) were fractured in the preparation chamber at a specimen temperature of -130°C and kept in the fully frozen hydrated state. Then they were transferred uncoated into the SEM and, still cooled to -130°C, observed at 2.1 kV in the SEM (Figs. 7a and 9a). Raising the stage temperature to -105°C, or -110°C respectively, causes specimen water to start to sublime. The progress of sublimation can be observed continuously in the SEM ("in situ etching", see Figs. 7b, 7c, 9b and 9c). Once the desired etching depth had been attained (independent of theoretically calculated times which are only valid for pure ice and a flat surface) the specimens were withdrawn to the cold stage of the preparation chamber (kept at -130°C, where sputter-coating with gold was immediately performed. The coated specimens were then returned to the SEM for final observation and recording at a temperature of -130°C and an acceleration voltage of 15 kV (Figs. 8; 10).

Large segregation patterns have been induced by slow freezing. Spruce needles were plunged in to liquid nitrogen and fractured after transfer into the preparation chamber. The segregation patterns produced by the ice crystal growth during freezing have a clearly defined, step-wise appearance during in situ etching. In contrast, low-fat dairy spread, fast frozen by plunging in to liquid propane, shows very fine segregation patterns (Fig. 9, 10). Only small regions of the water droplets display the effects of etching (Fig. 9c, arrowheads). Also, a smoothing out of the cross fracture of water droplets was observed during in situ etching.

Increasing deformation of big crystals, or disappearance of small ice crystals (circles) with time also indicates sublimation of water. The structural resolution is considerably improved by the coating of the specimens and the use of a higher acceleration voltage.

Planar Magnetron Sputter Coating

In freeze-etching for TEM, electron beam evaporation coating is applied in a high vacuum chamber, atoms move linearly (mean free path at 10^{-5} mbar $\sim$ 5 m) from the point-like source to the surface or fracture face of the specimen. This results in variations in heavy metal thickness which produces different contrast in the TEM. To complete the replication this coat is stabilized by a thick layer of evaporated carbon. The cleaning and transfer of these replicas has often proved to be problematic. Numerous techniques have been developed to increase the stability of replicas [e.g. DeMazière et al., 1985; Steere and Erbe, 1983; Stolinski et al., 1983]. In SEM a continuous specimen coating is required if the surface is to be electrically conductive. To attain this, specimens must be rotated or even tumbled during coating by electron beam evaporation [Amrein et al., 1990; Hermann et al., 1988], ion beam sputtering [Clay and Peace, 1981; Jakopic et al., 1978] or penning sputtering [Peters, 1980]. In cryo-preparations, the specimen temperature is crucial (see freeze-etching). Because of this, we prefer to keep our specimens in a fixed position during coating. In planar magnetron sputtering, atoms of the coating material originating from the extended target (mean free path at 10^{-2} mbar $\sim$ 5 mm, distance from target to specimen $\sim$ 70 mm) are scattered many times before reaching the specimen with different angles of incidence, therefore the whole surface is coated uniformly and the specimen can be kept at a well defined temperature.

The hexagonally arranged transmembrane protein arrays, found on the plasmatic fracture face (PF) of the plasmalemma of yeast (Saccharomyces cerevisiae), are good test specimens to evaluate the quality of freeze-etch preparations in TEM [Matile et al., 1969; Gross et al., 1978a]. At low voltages, however, we were never able to visualize these structures on uncoated samples in LTSEM [Walther et al., in press]. As it is necessary to coat specimens for high resolution LTSEM, we studied different coating materials.

Gold is frequently used for ambient temperature SEM, when only moderate resolution is required. Since a coating is indispensable and film thickness limits resolution, we sputtered a 3-4 nm gold layer onto a freeze-fractured yeast cell suspension (Fig. 11). Micrographs, recorded with a field emission SEM clearly show islands of gold on the PF of the yeast plasmalemma. The expected hexagonal arrays of volcano-like transmembrane proteins [Gross et al., 1978a] are hidden by these gold clusters, the para-crystalline arrays with a known lattice constant of 16.5 nm cannot be resolved

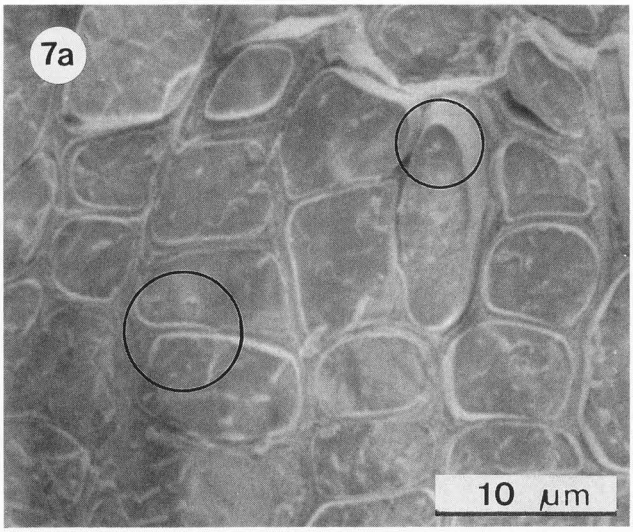

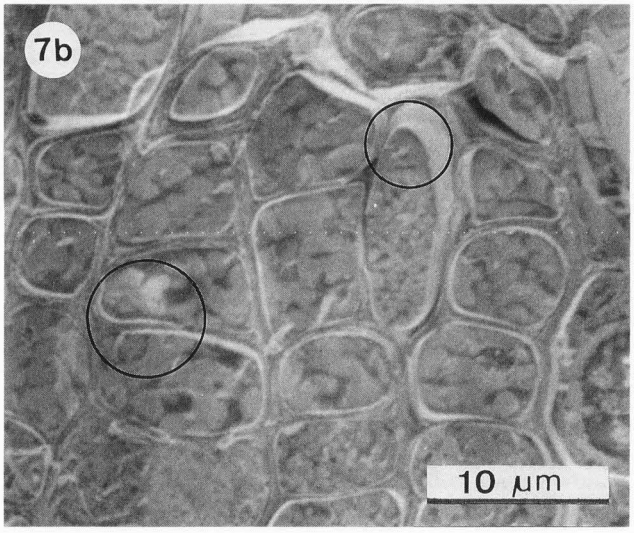

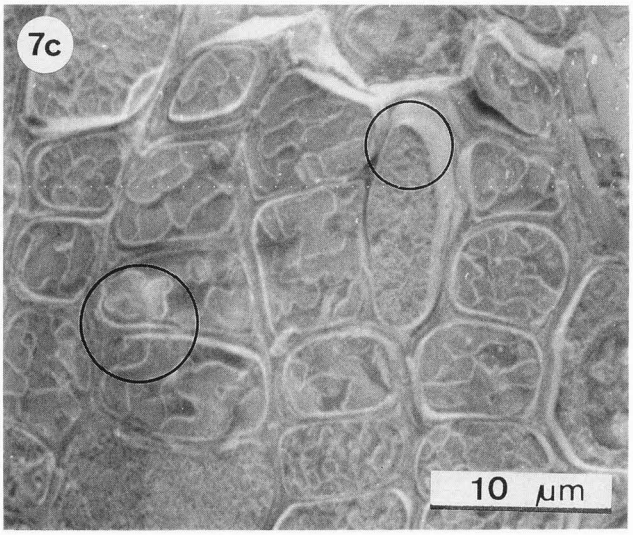

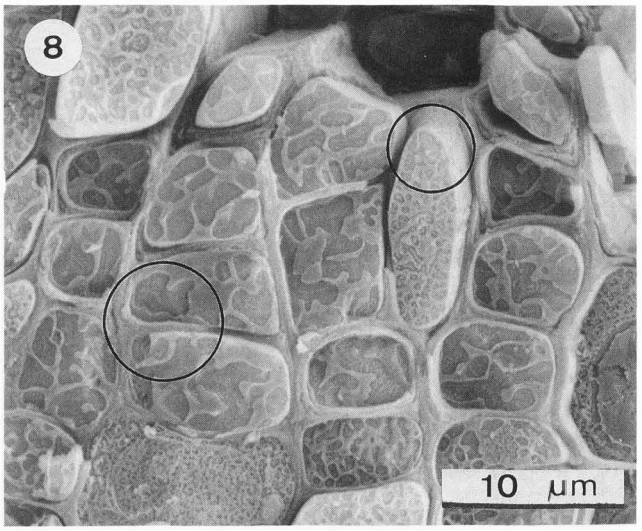

Figure 8 (above). Cross fracture through spruce needle (see Fig. 7 at left). Partially freeze-dried specimen, coated with 10 nm gold. Coating eliminates surface charging and allows water containing compartments to be identified. Note the improved structural resolution on the coated specimens. Acceleration voltage 10.4 kV.

Figure 9 (at right). Cross fracture through a water droplet in low-fat dairy spread. Uncoated specimen, accelerating voltage 2.1 kV.

Figure 9a. Sample fully frozen-hydrated, -110°C just reached. The fracture plane appears to be rough. Two ice crystals originating from fracturing are visible (circle).

Figure 9b. Sample partially freeze-dried for 4 minutes at -110°C. Due to the good freezing, the segregation pattern is too fine to show up on uncoated specimen.

Figure 9c. Sample partially freeze-dried for 10 minutes at -110°C. A smoothing out of the fracture plane is remarkable. Only few segregation structures are visible (arrowheads), but the deformation of the large and the disappearance of the small ice crystal (circle) prove that sublimation took place.

Figure 7 (at left). Cross fracture through a spruce needle of Picea abies. Uncoated specimen, accelerating voltage 2.1 kV.

Figure 7a. Sample fully frozen hydrated, -105°C just reached. The fracture plane appears to be smooth. Some ice crystals originating from fracturing are visible (circles).

Figure 7b. Sample partially freeze-dried for 5 minutes at -105°C. The segregation pattern, due to slow freezing, starts to appear by in situ etching.

Figure 7c. Sample partially freeze-dried for 15 minutes at -105°C. Ice crystals from fracturing are sublimed (circles). Etching depth is judged to be sufficient.

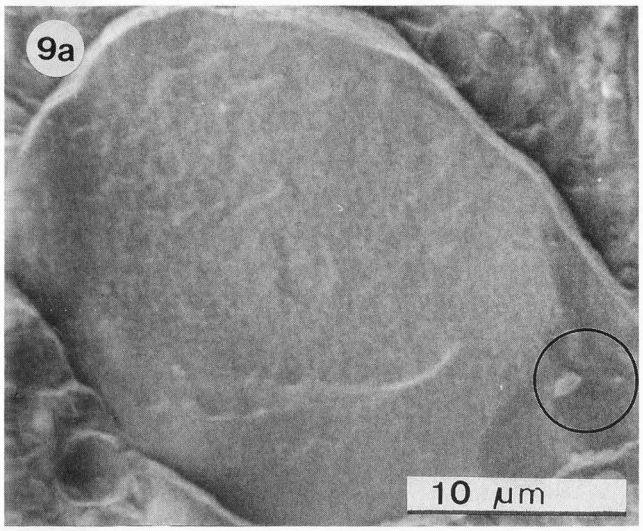

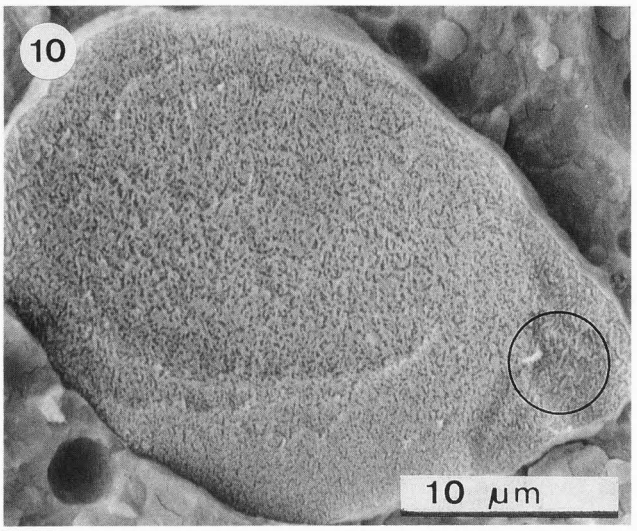

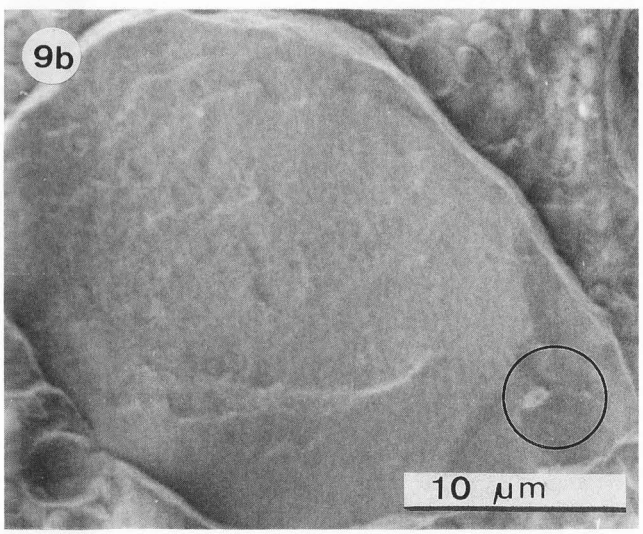

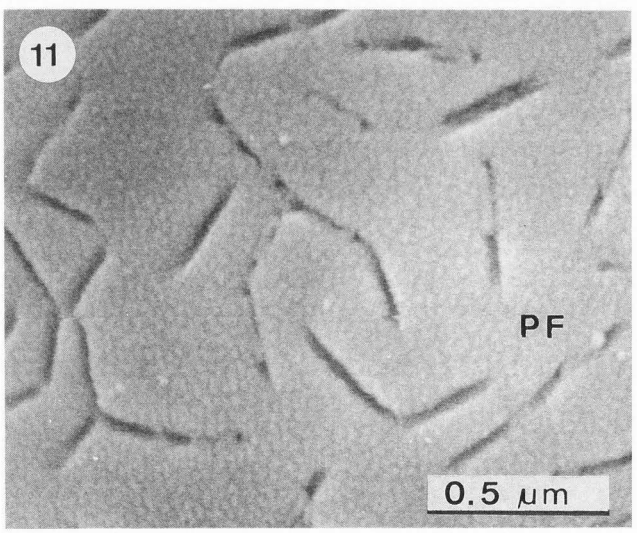

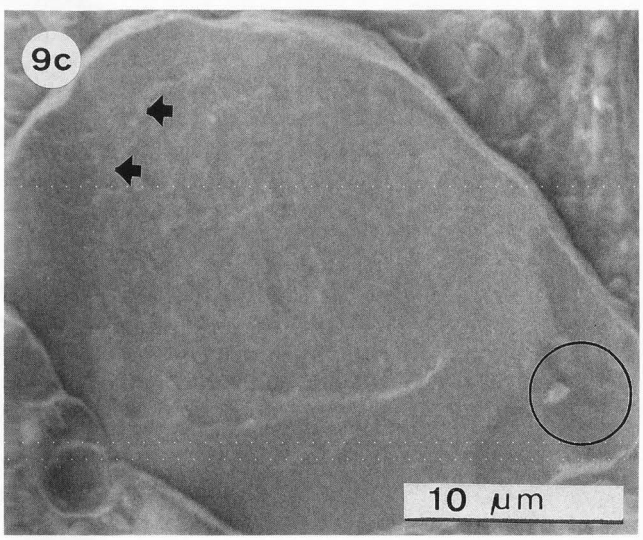

Figure 10. Cross fracture through low-fat dairy spread (see Fig. 9, at left). Partially freeze-dried specimen, coated with 10 nm gold. Thanks to the improved resolution by coating and 10.4 kV accelerating voltage, the fine segregation pattern is now visible, proving the identification of the water droplet.

Figure 11. Plasmatic fracture face (PF) of yeast plasmalemma coated with 3-4 nm gold. The gold islands are similar in size and distributed statistically, forming a coat on the membrane fracture face. The hexagonal arrays cannot be seen.

---

by gold coating. A series of coating layers were produced with different materials (Au, Au-Pd, Pt, Ta, Cr, W, see Fig. 12) in a low vacuum sputter-coater (SCD 040, Balzers). When imaged in TEM, platinum gives the highest contrast and the finest granularity for films with a nominal thickness of 0.4 nm.

Three films of platinum with different thicknesses were sputtered in a low vacuum chamber ($p >= 1 \times 10^{-2}$

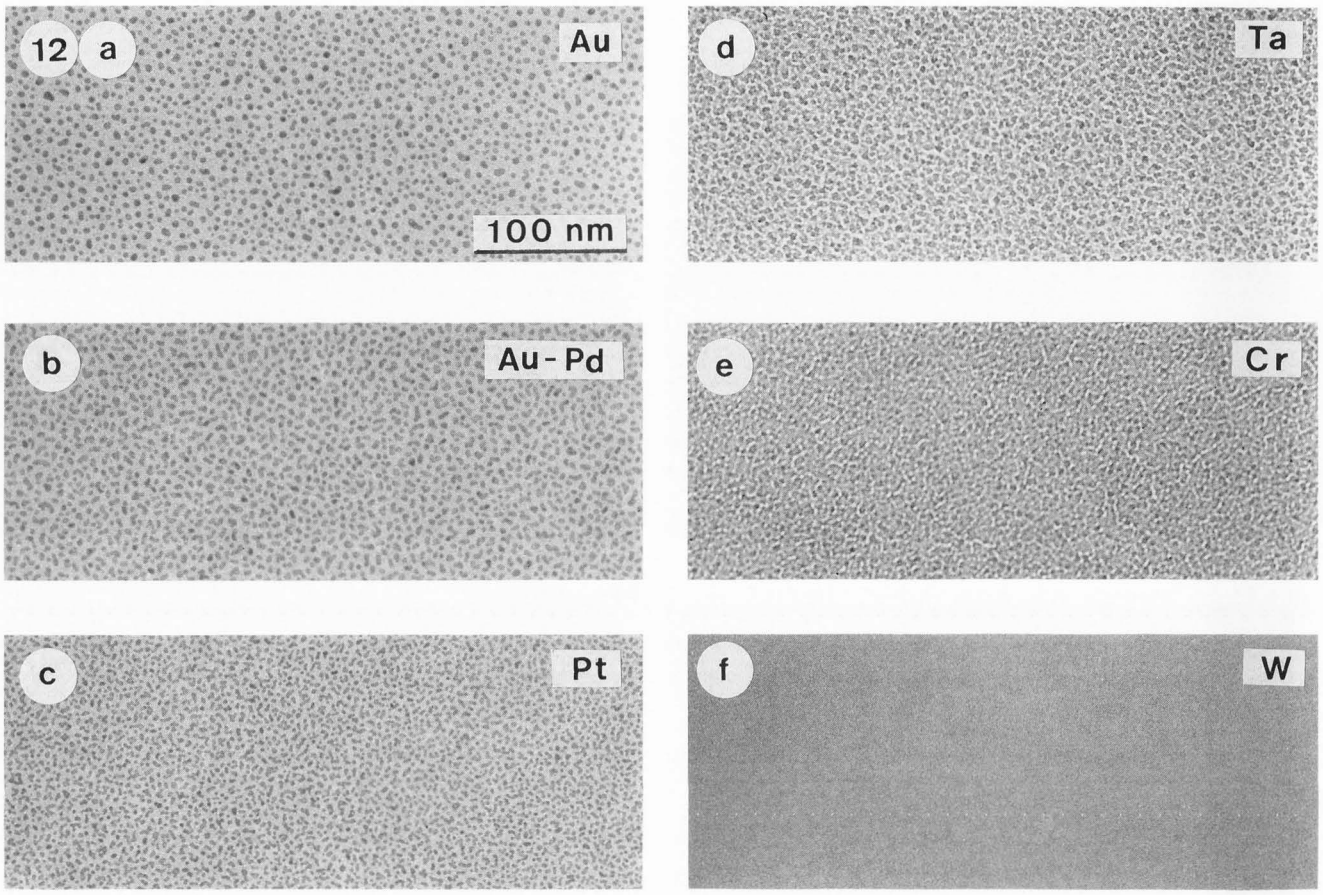

Figure 12. TEM micrograph of 0.4 nm (nominal film thickness) planar magnetron sputter coatings on carbon coated grids. Coatings were produced at room temperature and low vacuum conditions (SCD 040). Platinum (**c**) shows finer grains than gold (**a**) or gold-palladium (**b**). Chromium (**e**) is finer than tantalum (**d**), but contrast in TEM is less than that for platinum (**c**). Tungsten (**f**) is grainless due to oxidation.

mbar) keeping the specimens (carbon coated TEM grids) at room temperature (Fig. 13). The classical growth of a thin metal film can be watched in TEM. The three typical steps of single grain formation, coalescence of single grains to "worm-like" structures, and the formation of islands are visualized [Neugebauer, 1970].

From shadowing techniques in TEM, it is known that the specimen temperature influences the condensation behaviour of evaporated platinum-carbon [Gross et al., 1984; Müller, 1986, 1988]. As claimed by earlier authors [Zinsmeister, 1965], thinner continuous films are to be expected at lower temperatures due to reduced surface mobility of the metal atoms. Low temperature experiments should be performed under high vacuum conditions. Platinum sputtering with the same thicknesses as before was performed in a high vacuum chamber equipped with a Meissner cold trap (SCU 020, Balzers). After evacuation to a vacuum $<= 1 \times 10^{-5}$ mbar, the working pressure of 2.2×10^{-2} mbar was established with pure argon gas. Results of TEM examination of these samples (Fig. 14), compared with those conventionally obtained under low vacuum conditions (Fig. 13), shows that there is a considerable shift towards coalescence at thinner film thicknesses. The growth of particle-like structures on top of the platinum islands can be observed too.

Low temperature experiments were then carried out at -80°C under comparable high vacuum conditions (SCU 020, Balzers). Again the same nominal thicknesses of platinum were deposited on carbon coated grids (Fig. 15). As judged by TEM, a thin film of nominal thickness 0.4 nm already showed almost total coalescence. At 1.2 nm nominal film thickness, some granular structures are recognized on top of the thin platinum layer. At 4.0 nm, island formation has taken place, but between the islands the structure of the thin platinum film is still visible.

Thus, it is possible to obtain almost homogeneous platinum films by planar magnetron sputtering at specimen temperatures of -80°C or below, if a high vacuum chamber equipped with a Meissner cold trap is used (Müller and Walther, 1989).

Film Thickness and Accuracy of its Measurement

Fine structure, present on the surface of a specimen may be masked by a thick coating layer and, thus, cannot be resolved (Peters, 1985). At 10 kV acceleration voltage, for

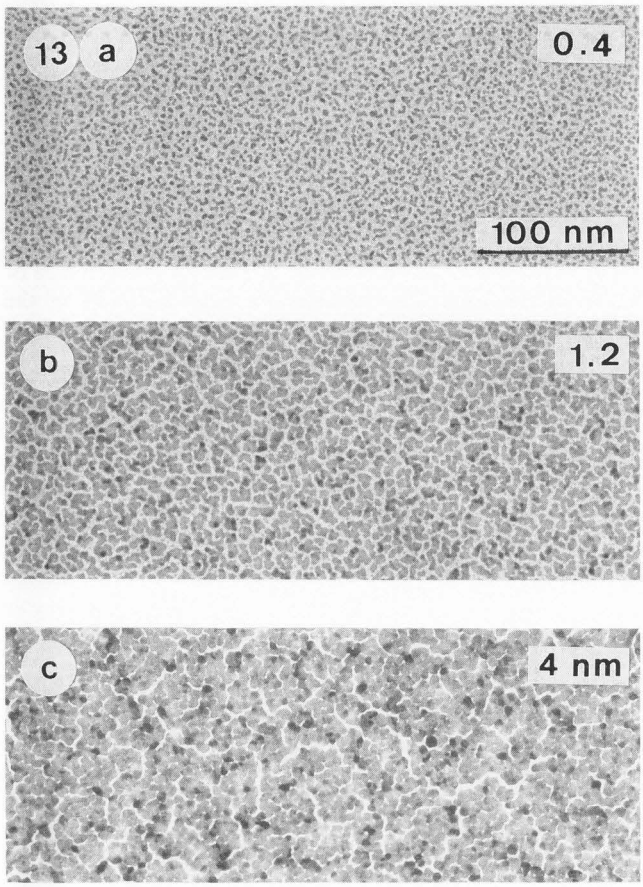

Figure 13. TEM micrographs of platinum films made by planar magnetron sputtering at low vacuum conditions and specimen at room temperature (SCD 040). For interpretations see text. Numbers at top right indicate nominal film thickness.

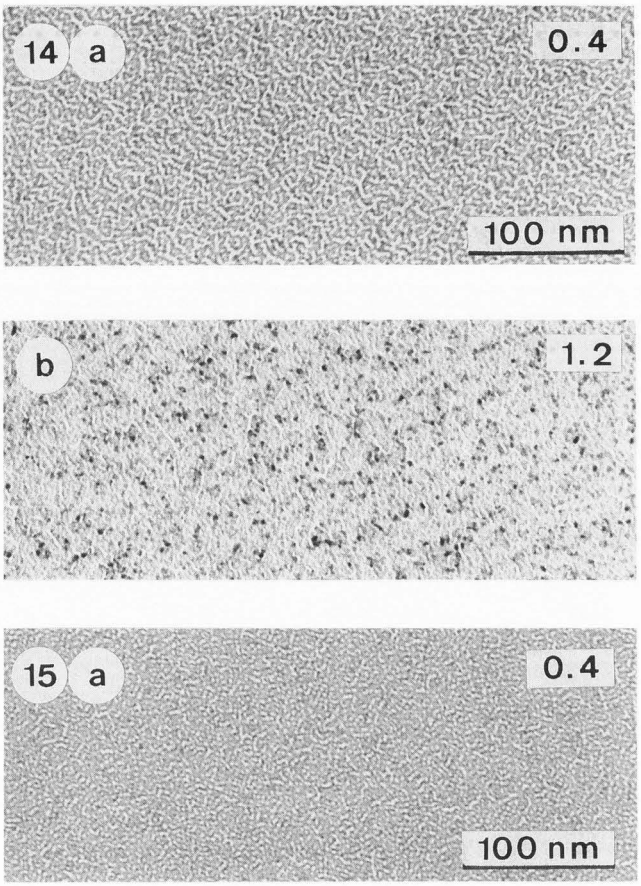

Figure 14 (top right). TEM micrographs of platinum films made by planar magnetron sputtering at high vacuum conditions (with Meissner cold trap) and specimen at room temperature (SCU 020). For interpretations see text. Numbers at top right indicate nominal film thickness.

---

example, the beam diameter of the primary electrons is estimated to be about 3.5 nm in our field emission SEM. Consequently, a coating layer of 1 to 3 nm thickness will not limit the sample resolution.

Planar magnetron sputter coating of nominally 2 nm platinum was applied to a freeze-fractured suspension of yeast cells (since the specimen was not completely flat, a thicker film was chosen). SEM micrographs (Fig. 16) show the presence of hexagonally arranged transmembrane proteins on the plasmatic fracture face (PF) (Walther et al., in press). In the center of these particles a dark point is visible. It is not yet clear whether this is the visulization of the depression (having a diameter of about 4 nm) known to exist in this structure (Gross et al., 1978a; Müller, 1986) or just due to the brightening of the flanks of the particles by the edge effect. Regardless, the resolution achieved is better than 10

Figure 15. TEM micrographs of platinum films made by planar magnetron sputtering at high vacuum conditions (with Meissner cold trap) and specimen at -80°C (SCU 020). For interpretations see text. Numbers at top right indicate nominal film thickness.

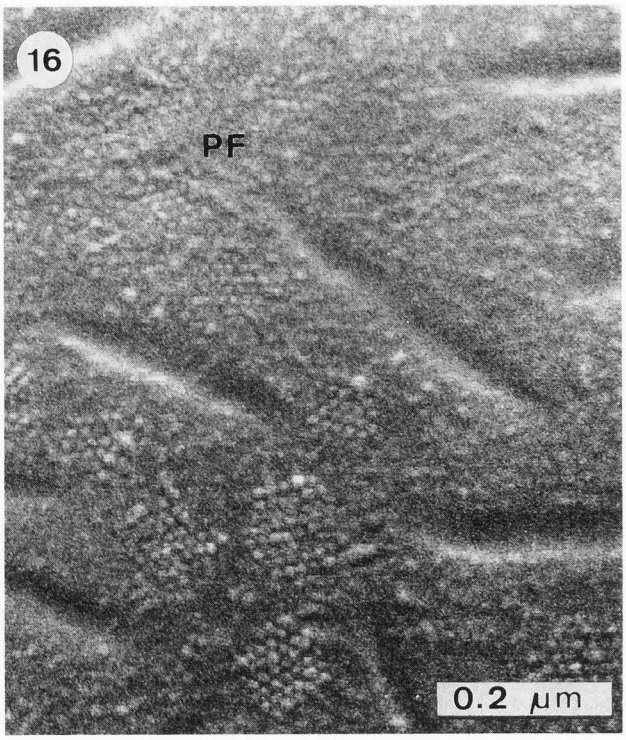

Figure 16 (left, top). Plasmatic fracture face (PF) of yeast plasmalemma, coated with nominally 2 nm Pt by planar magnetron sputtering at -110°C. Several of the hexagonally arranged transmembrane proteins show a black point in the center.

Figure 17 (left, bottom). Part of a cross fractured yeast cell prepared as for Fig. 16. Note the different distribution of intra-membrane proteins on exoplasmatic inner membrane (EFI) and plasmatic outer membrane (PFO) fracture face of the nucleus, and the plasmatic fracture face (PF) of the vacuole.

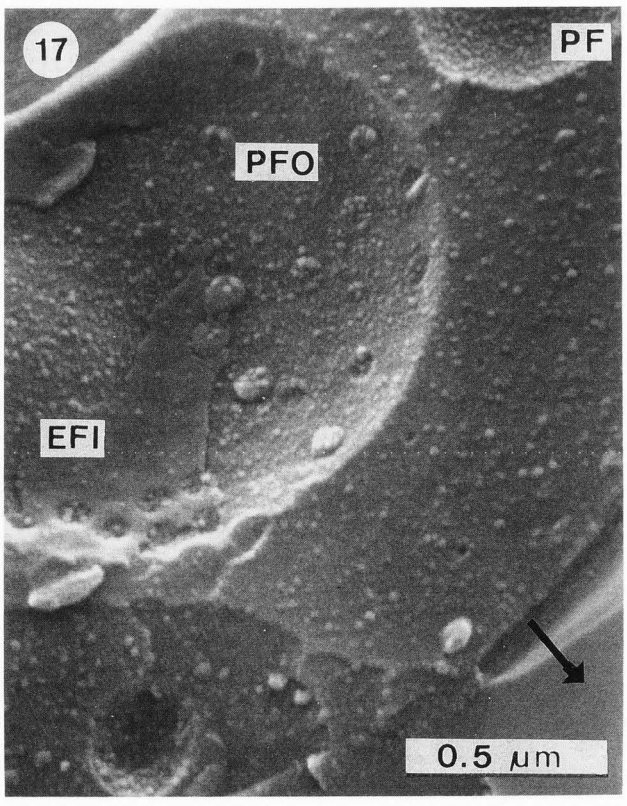

Table 1. Comparisons for platinum sputter coatings in high vacuum at -80°C

a: nominal film thickness, nm (quartz signal)	b: geometrically corrected film thickness, nm	c: STEM determined film thickness, nm*
0.4	0.8	0.9 (± 0.1)
1.2	2.4	2.4 (± 0.4)
4.0	8.0	5.3 (± 0.9)

*standard deviation in parentheses.

nm, because the space between the resolved particles (diameter ~ 13 nm) is ~ 4 to 5 nm (Müller, 1986).

Micrographs, such as Fig. 17, indicate that structural resolution was not limited by the coating layer. No structural details of the coating can be resolved on the ice surrounding the cross fractured yeast cell (arrow). The different density in the distribution of transmembrane proteins in the exoplasmatic inner membrane (EFI) and the plasmatic outer membrane fracture face (PFO) of the nucleus, as well as the membrane fracture step between, are clearly visible on Fig. 17 (Walther et al., in press). Many transmembrane proteins are visualized on the PF of the adjacent vacuole.

As it was possible to resolve these small structures on the fracture faces of our test specimen, it is now interesting to know the thickness of the coating layer. This thickness was measured by both quartz crystal and STEM (cf. Table 1). The nominal film thickness obtained by quartz crystal measurement was corrected by two factors taking into account the relative geometric positions of the source, the sample and the quartz crystal:

(i) In the horizontal direction a decrease in the sputter-coat thickness by a factor of approximately 2/3 was estimated by comparing the experimental values at the sites of the quartz crystal and the sample, i.e., a correction factor of 3/2.

(ii) In the vertical direction the thickness of the coating film changes approximately by the square of the distance from target to the sample (checked for low voltage sputtering, e.g. 320 V,and a working pressure of 2.2×10^{-2} mbar). Taking into account the positions of sample and

quartz crystal one can compensate for this dependence in our experimental set-up by a factor of 4/3. This gives a total geometric correction of 2, i.e., the actual coat thickness on a flat specimen is twice the nominal film thickness.

In the case of STEM measurements, the fraction of scattered electrons averaged over an area of approximately 1 μm^2 was converted into film thickness using a graph based on Monte Carlo calculations (taking the density of platinum to be 21.4 g/cm^3) [Reichelt and Engel, 1984]. The contribution of the thin carbon support film was subtracted.

The thickness estimates are in excellent agreement for the two thinner films (cf. column b and c in Table 1). A TEM micrograph of the thinnest platinum film (Fig. 15a) shows that an almost homogeneous layer, i.e., a solid metal coat is attained. This would seem to justify the assumption of bulk platinum density in the Monte Carlo calculations for these thicknesses. However, there is discrepancy of roughly 1/3 between the estimates for the thick film (4.0 nm, Fig. 15c) investigated. It is known from high resolution SEM work on cross fractured coatings (Nagatani et al., 1989) that magnetron-sputtered platinum films are approximately 3.2 times thicker than indicated by the quartz signal (film thickness in Nagatani's paper ranged from 17 to 64 nm).

This means that the mean density of the column-like structured coating is approximately 3 times lower than that of the solid metal. The TEM micrograph of our thick film Fig. 15c) indicates that such column-like structures are already present. This may introduce different systematic errors in both of the measurement methods used. Moreover, the structure of the sputtered platinum films on the carbon-foil (used for STEM) and on the quartz crystal may also vary resulting in different thickness estimations.

To conclude, a planar magnetron sputtered platinum film of approximately 1 nm in thickness appears almost homogeneous and allows details of freeze-etched biological specimens close to the resolution level of freeze-etch replicas for TEM (3-5 nm) to be visualized. Due to the high density of these coating films a high signal-to-noise ratio may be expected in the SEM which makes such platinum layers suitable for low temperature SEM at high resolution.

Conclusions

We visualized transmembrane proteins in frozen fixed bulk specimens which had not been exposed to any chemical treatment. Hexagonal arrays on the plasmatic fracture face of the yeast plasmalemma, well characterized by TEM investigations of freeze-etch replicas, were used as test specimens. The structural resolution achieved by low temperature field emission SEM at 10 kV was estimated to be better than 10 nm. The technique of multiple fracturing of frozen specimens in food research together with etching and coating of relatively large samples combined with high resolution low temperature SEM enables the continuous observation of freeze-fractures in low temperature SEM.

Acknowledgements

The authors wish to thank all the technical assistants in the institutes involved in this paper.

References

Amrein M, Dürr R, Winkler HP, Travaglini G, Gross H (1990) STM of freeze-dried and Pt-Ir-C-coated bacteriophage T4 polyheads. J. Ultrastruct. and Molec. Struct. Res. 102: 170-177.

Bachmann L, Schmitt-Fumian WW (1971) Improved cryo-fixation applicable to freeze-etching. Proc. Natl. Acad. Sci. USA 68: 2149-2152.

Bastacky J, Wodley C, LaBrie R, Backhus C (1987) A bibliography of low temperature scanning electron microscopy (LTSEM, Cryo-SEM) and scanning electron microscopy of frozen hydrated biological specimens. Scanning 9: 219-225.

Beckett A, Porter R, Read ND (1982) Low temperature scanning electron microscopy of fungal material. J. Microscopy 125: 193-199.

Böhler S (1975) Artifacts and specimen preparation faults in freeze etch technology. Balzers Publication No. DN 6573.

Brooker BE (1988) Low temperature methods in electron microscopy for food research. Hitachi Instrument News 14: 17-21.

Buchheim W (1982) Aspects of sample preparation for freeze-fracture/freeze-etch studies of proteins and lipids in food systems. A review. Food Microstructure 1: 189-208.

Buchheim W, Dejmek P (1990) Milk and dairy-type emulsions. In: Food emulsions, 2nd ed. Larson K, Fridberg S (eds.) Marcel Dekker, New York. pp. 203-246.

Clay CS, Peace GW (1981) Ion beam sputtering: An improved method of metal coating SEM samples and shadowing CTEM samples. J. Microscopy 123: 25-34.

DeMazière AMGL, Aertgeerts P, Scheuermann DW (1985) A modified cleansing procedure to obtain large freeze-fracture replicas. J. Microscopy 137: 185-188.

Dubochet J, Lepault J, Freeman R, Berryman JA, Homo JC (1982) Electron microscopy of frozen water and aqueous solutions. J. Microscopy 128: 219-237.

Dubochet J, Adrian M, Chang JJ, Homo JC, Lepault J, McDowall AW, Schultz P (1988) Cryo-electron microscopy of vitrified specimens. Quart. Rev. Biophys. 21: 129-228.

Echlin P (1981) Recent advances in specimen coating techniques. Scanning Electron Microscopy 1981;I: 79-90.

Echlin P (1985) Very low voltage sputter coating. J. Microscopy 137: 155-169.

Grabski C, Guggenheim R, Lüönd G, Düggelin M, Müller T (1987) Plant pathogenic fungi observed in SEM equipped with the SCU 020 cryo-preparation unit. Euro. J. Cell Biol. Suppl. 19(4): 19 (abstract).

Gross H, Bas E, Moor H (1978a) Freeze-fracturing in ultrahigh vacuum at -196°C. J. Cell Biol. 76: 712-728.

Gross H, Kübler O, Bas E, Moor H (1978b) Decoration of specific sites on freeze-fractured membranes. J. Cell Biol. 79: 646-656.

Gross H, Müller T, Wildhaber I, Winkler H, Moor H (1984) Fracturing and replication at -260°C. Proc 42nd Ann. Meeting EMSA, San Francisco Press, CA. pp 12-15.

Gross H, Müller T, Wildhaber I, Winkler HP (1985) High resolution metal replication, quantified by image

processing of periodic test specimens. Ultramicroscopy 16: 287-304.

Guggenheim R, Düggelin M, Mathys D, Grabski C (1991) Low temperature SEM for detection of fungicide activity. J. Microscopy, in press.

Harreveld A van, Crowell J (1964) Electron Microscopy after rapid freezing on a metal surface and substitution fixation. Anat. Rec. 149: 381-385.

Hermann R, Pawley J, Nagatani T, Müller M (1988) Double-axis rotary shadowing for high-resolution scanning electron microscopy. Scanning Microscopy 2: 1215-1230.

Heuser JE (1977) Quick-freezing to catch the membrane changes that occur during exocytosis. In: Proc. 35th Ann. Meeting EMSA, Claitor's Publishing Div., Baton Rouge, 676-679.

Honig RE, Hook HO (1960) Vapor pressure data for some common gases. R C A Review: 360-368.

Jakopic E, Brunegger A, Essl R, Windisch G (1978) A sputter source for electron microscopic preparation. In: Electron Microscopy 1978, Microscopical Society of Canada, Toronto. Vol. I: 150-151.

Jeffree CE, Read ND, Smith JAC, Dale JE (1987) Water droplets and ice deposits in leaf intercellular spaces: Redistribution of water during cryo-fixation for scanning electron microscopy. Planta 172: 20-37.

Matile P, Moor H, Robinow CF (1969) Yeast cytology. In: The yeasts, Rose AH, Harrison JS (eds.). Vol. I: 220-297.

Moor H (1959) Platin-Kohle-Abdruck-Technik angewandt auf den Feinbau der Milchröhren (Platinum-carbon replica technique applied to the fine structure of milk tubes). J. Ultrastruct. Res. 2: 393-422.

Moor H, Riehle U (1968) Snap freezing under high pressure: A new fixation technique for freeze-etching. In: Electron microscopy 1968. Proc. 4th Euro. Conf. Electron Microscopy, Tipografia polyglotta Vaticana, Rome, Vol. 2, 33-34.

Moor H (1971) Recent progress in the freeze-etching technique. Phil. Trans. R. Soc. London Ser. B: 261, 121-131.

Moor H (1986) Recent progress in high pressure freezing. In: Electron Microscopy 1986. Proc. 11th Int. Congr. Electron Microscopy, Kyoto. Japan Society of Electron Microscopy, Tokyo, Vol III: 1961-1964.

Müller M, Meister N, Moor H (1980) Freezing in a propane jet and its application in freeze-fracturing. Mikroskopie (Wien) 36: 129-140.

Müller T (1986) High resolution imaging of biological surfaces and fracture faces using cryo-preparation and grainless shadowing. Dissertation at Swiss Fed. Inst. of Technology (ETH), Zurich. No. 8053.

Müller T, Guggenheim R, Düggelin M, Lüönd G (1986) On-line cryo-preparation and cryo-microscopy in SEM with SCU 020. In: Electron Microscopy 1986. Proc 11th Int. Congr. Electron Microscopy, Kyoto. Vol III: 2233-2234.

Müller T (1988) Freeze-fracturing and shadowing at -110°C and -260°C. In: Electron Microscopy, 1988, Proceedings IV Asia-Pacific Conference and Workshops, The Electron Microscopy Society of Thailand, Bangkok. 361-366.

Müller T, Guggenheim R, Düggelin M, Mestres P, Van Aelst AC, Heyser W, Kumpfer W (1988) Freeze-etching and cryo scanning electron microscopy (CSEM) of plant and animal tissues with SCU 020. In: Proc Euro. E.M. Congress 1988, Inst. Phys. Conf. Ser. No. 93, 3: 15-16.

Müller T, Walther P (1989) Thin films for high resolution low temperature SEM. In: Proc Scanning 89/EM West. FACM Inc. Mahwah, NJ. 208-209.

Müller T, Guggenheim R, Düggelin M, Scheidegger C (1991) Freeze-fracturing for conventional and field emission low temperature scanning electron microscopy: The scanning cryo unit SCU 020. J. Microscopy, in press.

Nagatani T, Suzuki T, Yamada M, Nakagawa M (1989) Film thickness measurement by cross-sectional SEM. Proc. 47th Ann. Meeting EMSA, San Francisco Press, 728-729.

Neugebauer CA (1970) Condensation, nucleation, and growth of thin films. In: Handbook of Thin Film Technology Maissel LI, Glang R (eds.). McGraw Hill, New York, Chapter 8.

Peters KR (1980) Penning sputtering of ultra thin films for high resolution electron microscopy. Scanning Electron Microscopy 1980;I: 143-153.

Peters KR (1985) Working at higher magnifications in scanning electron microscopy with secondary and backscattered electrons on metal coated biological specimens and imaging macromolecular cell membrane structures. In: The Science of Biological Specimen Preparation for Microscopy and Microanalysis 1985. Müller M, Becker RP, Boyde A, Wolosewick JJ (eds.), Scanning Electron Microscopy Inc AMF O'Hare, IL. 257-282.

Plattner H, Bachmann L (1982) Cryo-fixation: A tool in biological ultrastructural research. Int. Rev. Cytol. 79: 237-304.

Plattner H, Zingsheim HP (1983) Electron microscopic methods in cellular and molecular biology. In: Subcellular biochemistry, Roodyn DB (ed.), Plenum Press, New York. Vol 9: 1-236.

Read ND (1990) Low temperature scanning electron microscopy of fungi and fungus-plant interactions. In: Proc. Int. Symp. E.M. Applied in Plant Pathology, Springer Verlag, in press.

Reichelt R, Engel A (1984) Monte Carlo calculations of elastic and inelastic electron scattering in biological and plastic materials. Ultramicroscopy 13: 279-294.

Robards AW, Crosby P (1978) A transfer system for low temperature scanning Electron microscopy. Scanning Electron Microscopy 1978;II: 927-936.

Robards AW, Sleytr UB (1985) Low temperature methods in biological electron microscopy. In: Practical Methods in Electron Microscopy, Vol. 10, Glauert AM (ed.) Elsevier.

Sargent JA (1988a) Low temperature scanning electron microscopy: Advantages and applications. Scanning Microscopy 2: 835-849.

Sargent JA (1988b) The application of cold stage scanning electron microscopy to food research. Food Microstructure 7: 123-135.

Steere RL (1971) Retention of three dimensional contours by replicas of freeze-fracture specimens. Proc 29th Ann. Meeting EMSA, 242-243.

Steere RL, Erbe EF (1983) Supporting freeze-etch specimens with "Lexan" while dissolving biological remains in acids. Proc. 41st Ann. Meeting EMSA, 618-619.

Steinbrecht RA, Zierold K (Eds.) (1987) Cryo-techniques in Biological Electron Microscopy. Springer Verlag.

Stolinski C, Gabriel G, Martin B (1983) Reinforcement and protection with polystyrene of freeze-fracture replicas during thawing and digestion of tissue. J. Microscopy 132: 149-152.

Walther P, Hentschel J (1989) Improved representation of cell surface structures by freeze-substitution and backscattered electron imaging. Scanning Microscopy Supplement 3: 201-211.

Walther P, Hentschel J, Herter P, Müller T, Zierold K (1990) Imaging of intramembranous particles in frozen hydrated cells (Saccharomyces cerevisiae) by high resolution cryo SEM. Scanning, in press.

Zinsmeister G (1965) Beitrag zur Frenkel'schen Kondensationstheorie (Contribution to the Frenkel condensation theory). In: Proc. Int. Symp. Basic Problems in Thin Film Physics, Niedermayer R, Mayer H (eds.), Published by Vandenhoeck and Ruprecht, Goettingen, Germany, 33-42.

Discussion with Reviewers

J.A. Sargent: If the SCU 020 is cooled by liquid nitrogen, it should be possible to operate both cold stages at a temperature close to -180°C. At such temperatures, the vapor pressure of water is virtually zero and no condensation should occur onto the specimen during coating or examination. Why were the specimens fractured and observed at temperatures as high as -120°C? Was an anti-contaminator, maintained at low temperature, incorporated as a water vapor trap into the system?

Authors: The SCU 020 is indirectly cooled with liquid nitrogen via cold plates and copper stranded wires (see: Müller et al., 1991). At temperatures below -150°C the saturation pressure of water is less than 10^{-11} mbar (Honig and Hook, 1960), so in the vacuum of the preparation chamber or SEM (partial pressure of water $\sim 10^{-7}$ mbar) the rate of evaporation for a water molecule is 10^{-4}, but the rate of condensation is 10^{4} per second. An anti-contamination plate can only reduce the angle of straight moving water molecules originating from residual gas atmosphere for possible condensation, but cannot exclude the condensation completely. To reduce the risk of condensation, a higher specimen temperature, that is, a reduced condensation rate is the only possibility. Especially, the specimen temperature in the time between fracturing and coating is very critical, so we chose -110 to -120°C for frozen hydrated experiments in the preparation chamber (specimen temperature close to the critical condensation temperature, see text). In the SEM, just for observation of coated specimens, a lower temperature is appropriate to reduce beam damage (contamination is reduced by an anti-contamination plate).

A. Boekestein: You mentioned that after cryo-fixation the specimen was at -120°C for fracturing or was warmed up to -100°C for etching. Have you found any evidence of vitrified water transformed to the crystalline state in these experiments?

Authors: No, because we used simple freezing methods (plunging in to liquid nitrogen or propane). The segregation pattern visible in Figs 1, 2, and 6 to 10 is interpreted as a result of ice crystal formation during freezing. So we think these specimens never were vitrified.

A. Boekestein: Please elaborate on the immediate coating of the specimen after fracturing of a frozen biological object: Does it prevent the sublimation or does it prevent the condensation of water?

Authors: Coating is started already before fracturing the specimens. So, immediately after creation of the fracture, the coating layer is produced. Sublimation and condensation depend on vacuum and specimen temperature (see above), and are time related. By reducing the time of action, these processes can be limited by temperature, vacuum and immediate coating (no sublimation afterwards), but not excluded. For partially freeze-dried specimens the major event is sublimation which is stopped by the formation of a coating layer.

A. Boekestein: Do you advocate that examination of uncoated frozen biological fractured surfaces at low accelerating voltage just to avoid charging is the wrong solution for high resolution cryo-SEM?

Authors: Yes, we do. Comparing Figs. 7c and 8, or 9c and 10, one can see, that the structural resolution is enhanced by coating and use of higher accelerating voltage. Nevertheless, in situ etching, using low accelerating voltage, is useful when new, unknown specimens have to be observed.

A. Boekestein: Can the segregation pattern in Fig. 6 be regarded as an indication of the crystal size in the frozen specimen? What is the likely nature of the solid at the segregations?

Authors: It is not completely clear if we see individual ice crystals or fingers of dendrites of a large single ice crystal; there is evidence by electron diffraction, that in one cell just one ice crystal grows [Dubochet et al., 1988], but here we are looking at whipped cream. The material left behind after etching the pure water is interpreted as non-water material (fats, oils, sugars, salts, proteins...).

I. Heertje: In whipped cream no oil droplets were detected on the air-water interface. This is in contradiction with earlier observations (e.g., Schmidt DG, Food Microstruct. 1, 151, 1982, and Brooker BE, Food Microstruct. 5, 277, 1986). The stabilization of air cells in whipped cream is in general ascribed to the combined action of both a protein film and oil droplets at the interface. Can an explanation be offered for this discrepancy?

Authors: This observation must be due to a too short whipping of the cream (Buchheim, personal communication). Indeed the whipped cream was produced from a spray can. The "whipping", therefore, was caused by turbulence during spraying, which was done in a fraction of a second.

I. Heertje: Apparently, the size of water droplet in the low-fat spread is rather large (about 40 micrometers, Figs. 9, 10). Is this an average size? Could coalescence of water

droplets have been induced by the sampling procedure (1 mm samples)?
Authors: We carried out to few experiments to be able to determine influences of sampling or aging of this particular low fat spread. We did not investigate the role of the size of the water droplets.

K.-R. Peters: How were the frozen specimen cubes fixed under liquid nitrogen on to the specimen table?
Authors: The specimen were frozen together with a specimen support plate. This was then fixed on to the specimen table (interface support-cold stage) with a clamp spring or screwed in to the specimen table under liquid nitrogen.

K.-R. Peters: Can the high rate of ice crystal contamination observed in your cryo-fracturing/magnetron sputtering system be avoided through high vacuum deposition techniques, i.e., evaporation or ion beam sputtering?
Authors: The contamination shown in Figs. 3,4 was due to a too low specimen temperature (see discussion with J.A. Sargent, above). When fracturing is performed close to the critical condensation temperature, and immediate planar magnetron sputter coating is carried out (see discussion with A. Boekestein) very little contamination by water vapor occurred (bright particles in Fig. 16) and high resolution LTSEM can be carried out without the coating (shadowing) techniques you mention.

K.-R. Peters: How can ice crystal contamination be controlled on surfaces observed by in situ cryo-SEM before and after coating when transferred from high vacuum through the low coating vacuum back to high vacuum?
Authors: The partial pressure of water is always at high vacuum conditions ($<= 1 \times 10^{-6}$ mbar) due to the attached turbo molecular pump and the built in Meissner cold trap (see Müller et al., 1991). These conditions are maintained during in situ LTSEM, on-line high vacuum cryo transfers from and to the SEM, and coating with pure argon gas at 2.2×10^{-2} mbar. By monitoring the specimen temperature, therefore, the ice crystal contamination can be controlled. Accuracy of specimen temperature is $\pm$ 1°C.

K.-R. Peters: Is it theoretically allowed to apply, at multiple scattering conditions, the inverse square law for estimation of coating distributions? Do you assume that in cryo magnetron sputtering the number and composition of gas molecules and ions is homogeneous between the target and the specimen surface?
Authors: At the moment, we have little evidence of a continuity of the residual gas composition regarding ions and argon molecules between target and specimen. The inverse square law, we think, cannot be applied in general, but, as experimentally checked for low voltage coating (see text) and a total pressure of 2.2×10^{-2} mbar, we think it is a reasonable estimation.

K.-R. Peters: If you assume that the thin cryo magnetron sputtered platinum film (Fig. 15a) is continuous and allow for the interpretation of the thick film (Fig. 15c) as being discontinuous and provided with big cracks, then the change in film continuity may indicate serious coating damage and possibility for fine structural specimen damage.
Authors: We think that the bright areas between the dark platinum islands are not cracks. We observed in the bright areas of Fig. 15c the same structures as in Fig. 15a. Therefore, we interpret Fig. 15c as follows: On a more or less uniform, homogeneous layer of about 1 nm platinum, column-like structures grow. This could be explained with a changed affinity of the now platinum-covered surface to the platinum atoms arriving from the target. The columnar structures appear as islands in TEM, and because of their high contrast, the thin platinum layer is hardly visible. If no cracks are present, then no specimen damage can be expected, but small surface details may be hidden then.